Investigation of the Diffusion Process in Cross-Linked Polystyrenes by Means of NMR Imaging and Solid-State NMR Spectroscopy

Martin Ilg, Bettina Pfleiderer, Klaus Albert, Wolfgang Rapp, and Ernst Bayer*

Institut für Organische Chemie der Universität, Auf der Morgenstelle 18, D-72076 Tübingen, FRG

Received June 7, 1993; Revised Manuscript Received February 16, 1994®

ABSTRACT: The diffusion process of a solvent (dioxane) in samples of different cross-linked polystyrenes can be monitored by combined NMR imaging and solid-state NMR techniques. NMR imaging data reveal a strong dependence of the diffusion behavior upon the cross-link density: in the case of lowest cross-linking (1%), a case II diffusion process takes place, whereas in the case of highest cross-linking (5%), Fickian diffusion occurs. The 2.5% cross-linked polystyrene shows intermediate behavior. Solid-state NMR relaxation parameters indicate great differences between the unswollen and the swollen state. Whereas the relaxation data obtained in the unswollen state are almost independent of the degree of cross-linking, great differences are observed between the 1% and 5% cross-linked polymers in the swollen state, with both the highest overall mobility and, in particular, a high mobility of the phenyl group in the case of the 1% cross-linked material. This behavior can be directly related to the different types of diffusion, suggesting that the strong interaction of the highly mobile phenyl groups with the dioxane in the low cross-linked material favors case II diffusion. In the 5% cross-linked materials, with a lower overall mobility and no predominant high phenyl group motion, Fickian diffusion occurs. Increased cross-linking corresponds to increasing $T_{1\rho C}$ and T_{1C} values, thus indicating reduced mobility.

1. Introduction

Polymeric supports are helpful tools in many fields of application such as chromatography (e.g., reversed-phase and gel permeation chromatography),[1] as supports for catalysts[2] and enzymes,[3,4] as polymeric reagents,[5] and as ion exchangers.[6] With the development of the solid-phase peptide synthesis,[7,8] the use of insoluble polymeric supports has become common in chemical synthesis.

In all mentioned applications, surface interactions and diffusion are the most important processes for mass transport and exchange phenomena.

A common property of all supports is that the reagent has to penetrate the polymeric matrix. Inside the polymeric matrix, all transport processes are controlled by diffusion.[9] Thus, matrix parameters, such as matrix dimension, polarity, cross-linking, and matrix design (e.g., macroporous, microporous, or gelatinous),[10] determine the diffusion values[11] and influence the kinetics of the reaction.

We have applied nuclear magnetic resonance imaging (NMRI) as well as ^{13}C solid-state (*c*ross *p*olarization/*m*agic *a*ngle *s*pinning) NMR spectroscopy to obtain more detailed information about these phenomena.

NMRI is a noninvasive medical diagnostic method[12] which came to its full potential in the 1980s. It yields an image of the NMR intensity as a function of location in an object with the help of additional magnetic field gradients. The signal intensity is dependent on the local concentration of spins and their T_1 and T_2 relaxation times. It is possible to enhance one of these parameters in the image by appropriately adjusting the pulse imaging sequence. At present the technique is mainly used for the visualization of protons in liquid or gellike states.

The development of microimagers with high spatial resolution[13,14] led to increasing application of NMRI in materials science,[15-18] especially for studies of the diffusion of fluids in polymers[19-21] and the flow of fluids in packed beds.[22,23]

Polymeric systems, such as cross-linked polystyrenes, can be characterized by their dynamic parameters, obtained by ^{13}C high-resolution NMR spectroscopy[24,25] or ^{13}C CP/MAS NMR spectroscopy. Motions in polymers ascribed by the proton and carbon spin–lattice relaxation times in the rotating frame $T_{1\rho H}$ and $T_{1\rho C}$, respectively, and the carbon spin–lattice relaxation times in the laboratory frame T_{1C} have been studied extensively by solid-state NMR spectroscopy for many years.[26-28] For glassy polymers well below the glass transition temperature T_g such as polystyrene, local motions like side-chain motions, terminal group motions, or main-chain local fluctuations dominate the relaxation behavior,[25] whereas for polystyrene in the gel state above T_g, backbone motions contribute predominantly.[26,29,30]

For polymers below T_g, the megahertz motions reflected in T_{1C} do not describe the mechanical properties. Instead, the main-chain motions in the 15–100-kHz range are important.[26,31,32] $T_{1\rho H}$ and $T_{1\rho C}$ are sensitive to this frequency region. However, the $T_{1\rho H}$ values are averaged due to spin diffusion,[28,29] and the description of local dynamics is not possible. Thus, $T_{1\rho C}$ is the parameter of choice, though $T_{1\rho C}$ relaxation could be theoretically complicated by a competitive spin–spin relaxation pathway. Fortunately, this pathway has been shown to contribute only to a minor degree with polystyrene, and $T_{1\rho C}$ can be treated as a parameter describing the motion of polymer groups.[27,31] The determination of $T_{1\rho H}$ and $T_{1\rho C}$ thus allows the characterization of motions at frequencies comparable to that of the applied field (30–60 kHz) at different spectral densities.

Although a great deal of investigation has been carried out on polymer motions in the glassy amorphous state, only a few reports about the dynamics of polymer–solvent interactions have appeared.[30,33,34] One reason might be that cross-polarization (CP) in the gel state usually is an inefficient process, because the static dipolar interactions necessary for efficient CP are greatly reduced by the high mobility.[29,33,34] Due to the local motions, the spectra of

® Abstract published in *Advance ACS Abstracts*, April 1, 1994.

0024-9297/94/2227-2778$04.50/0

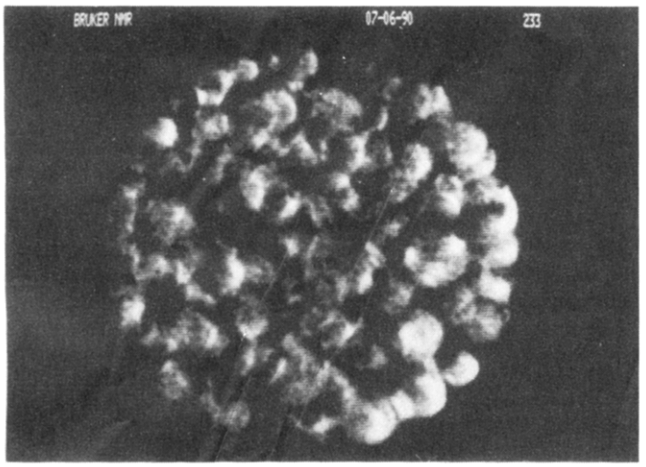

Figure 1. Spin–echo image of an array of polystyrene beads used in chromatography. The beads are swollen in dioxane and have a diameter of about 400 μm. Image parameters: slice thickness 180 μm, spatial resolution 23 μm, field of view 4 mm.

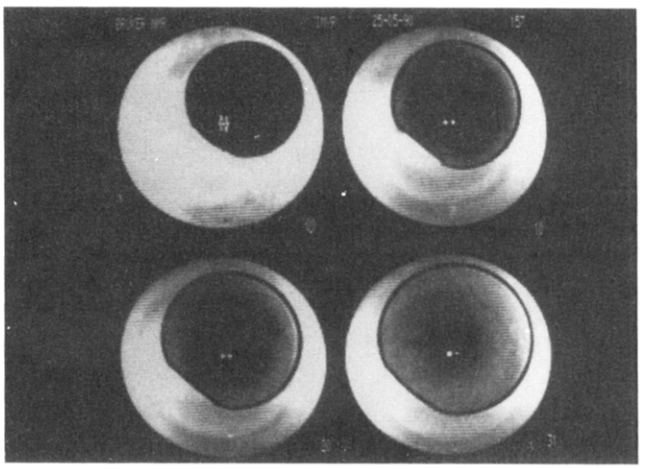

Figure 2. FLASH images of 8-mm polystyrene (2.5% cross-linked) cylinders upon exposure to dioxane. Image parameters: echo time 4 ms, repetition time 50 ms, 256^2 matrix, imaging time for one image 120 s, slice thickness 1.5 mm, spatial resolution 115 μm, field of view 28 mm.

swollen cross-linked polystyrenes have a less favorable signal-to-noise ratio relative to glassy dry samples and the C-1 phenyl peak at 146 ppm is barely visible.[33,34] Spectra suitable for evaluating relaxation data nevertheless can be obtained, and the other resonances of interest can be resolved and clearly seen. Therefore, the dynamic behavior of the unswollen and swollen polystyrenes can be correlated with the swelling dynamics and the diffusion process monitored by NMRI.

2. Methods

2.1. Sample Preparation. Styrene, technical divinylbenzene (DVB) with 33% ethylvinylbenzene, and dibenzoyl peroxide (BPO) were purchased from Merck (Darmstadt, FRG).

Styrene and DVB were mixed in the ratios 100:1, 100:2.5, and 100:5, and the radical initiator BPO was added. The mixture was transferred to a 30 cm × 8 mm diameter tube and polymerized at 100 °C for 24 h.

Swelling factors $f = V_s/V_d$ (V_s = volume swollen, V_d = volume dry) were determined by treating 1-cm rods of cross-linked polystyrene with dioxane for 5 days. The value of f varied between 1.4 and 2.5 for 5% and 1% cross-linked polystyrene, respectively.

2.2. NMR Imaging Experiments. Although it is possible to image the chromatographic beads themselves (Figure 1), the monitoring of the diffusion behavior and the homogeneity of the cross-linking requires bigger samples. For this reason, we made cylindrical-shaped specimens with a diameter of 8 mm, using the same material and methods as for the preparation of the beads. These samples are exposed to dioxane in test tubes at 50 °C and imaged on a Bruker MSL 200 NMR spectrometer equipped with a microimaging accessory. Unless otherwise noted, we used a rapid FLASH imaging sequence[37] that is based on a gradient echo. In addition to its short imaging time, it offers the possibility of adjusting the acquisition parameters in such a way that the signal is almost exclusively dominated by the spin density.[34] Moreover, we found FLASH to offer superior contrast in comparison to spin–echo sequences, due to its extremely short echo time.

A simulation of the signal intensity vs T_2 shows virtually no T_2 weighting for dioxane protons with a T_2 greater than 20 ms for the following optimal image parameters: tip angle 15°, gradient strength 5 G/cm, repetition time 50 ms, and echo time 4 ms. The image consisted of 256 × 256 pixels, and eight averages were coadded. This corresponded to an imaging time of 120 s, a slice thickness of 1.5 mm, and a spatial in-plane resolution of 115 μm in a field of view of 28 mm. To shorten T_1, the dioxane in the FLASH images was doped with 4 mg/mL of chromium-(III) acetylacetonate [$Cr(acac)_3$].

2.3. Solid-State NMR Experiments. The solid-state ^{13}C NMR measurements were carried out on the same Bruker MSL 200 NMR spectrometer at 4.7 T with samples of 200–300 mg in double-air-bearing rotors of ZrO_2 in a Bruker double-air-bearing MAS probe. Magic angle spinning was routinely carried out at 4-kHz spinning rates. Typically, the proton 90° pulse length was 5 μs and the repetition time 2 s. To eliminate experimental artifacts, block averaging was used to spread out the individual measurements over time. All ^{13}C NMR spectra were externally referenced to liquid tetramethylsilane.

The pulse sequences used have been described in detail elsewhere. The proton relaxation time in the rotating frame $T_{1\rho H}$ was measured as described by Schaefer et al. at a ^{13}C field strength of 32 kHz.[35]

The spin–lattice relaxation time T_{1C} was measured by a spin-temperature-alternated cross-polarization pulse sequence followed by a 90° phase-shifted $\pi/2-\tau-\pi/2$ ^{13}C pulse sequence.[36]

The contact times used were 1 ms (swollen polystyrene) and 3 ms (swollen polystyrene gels) for all relaxation measurements, and the temperature was adjusted to 300 K.

The polymers were allowed to swell in dioxane and packed in ZrO_2 rotors which were sealed according to Ford et al.[33,34]

3. Results and Discussion

3.1. Nuclear Magnetic Resonance Imaging (NMRI) Investigations. Figure 2 demonstrates four stages of the dioxane penetration in 2.5% cross-linked polystyrene. With this imaging technique the solid unswollen polystyrene does not yield any signal because of its extremely short T_2 and subsequently appears black. The surrounding bulk dioxane is bright, while the penetrating diffusion front shows up in different gray tones according to the dioxane concentration in the polymer matrix. Multicomponent diffusion between dioxane and $Cr(acac)_3$ may contribute to the susceptibility artifact observed, but the dark contour enhancement at the polymer–fluid

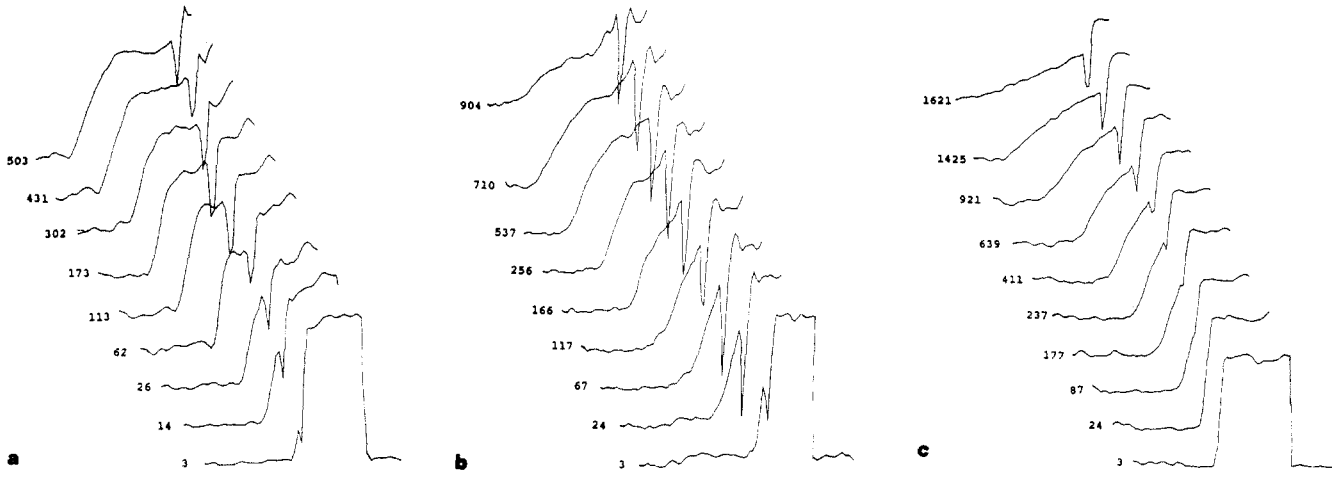

Figure 3. Stacked plot of the intensity profiles of different cross-linked polystyrene: (a) 1% cross-linked; (b) 2.5% cross-linked; (c) 5% cross-linked.

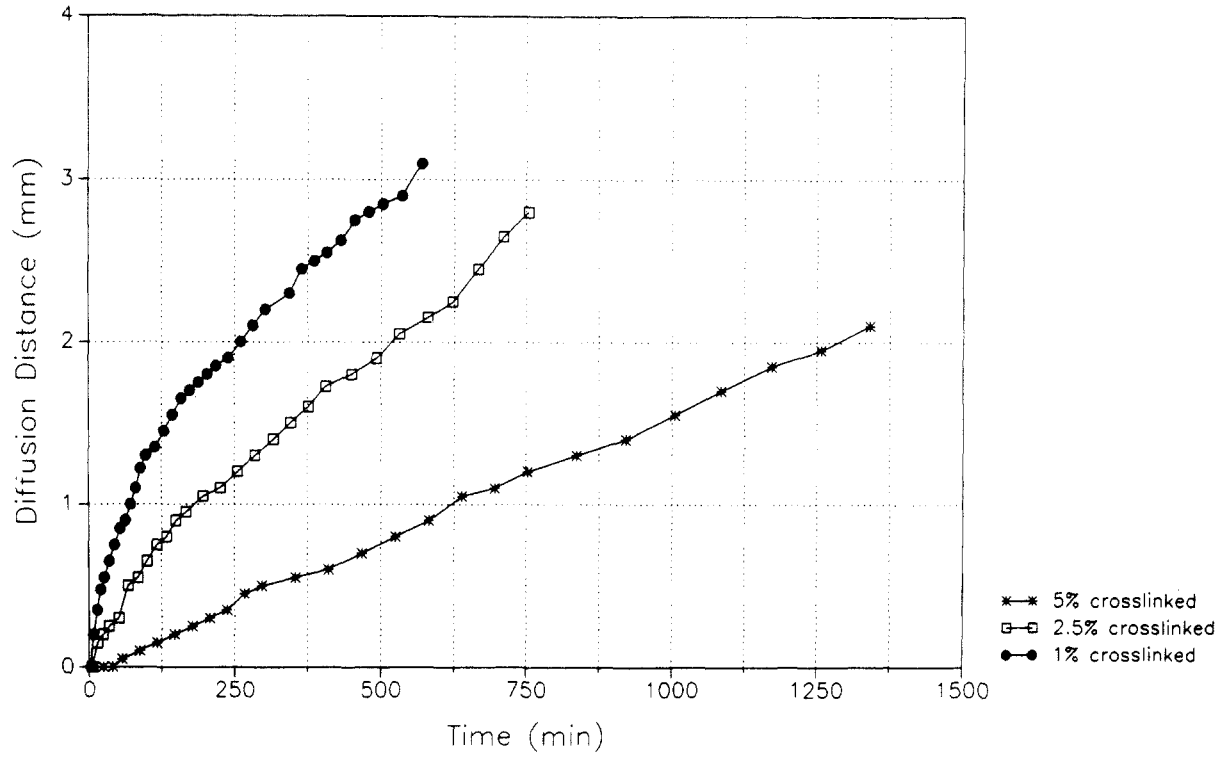

Figure 4. Plot of diffusion distance versus time.

borderline is mainly a magnetic susceptibility change. Susceptibility alterations are either due to a local concentration of Cr ions of the doped dioxane at the surface of the swollen polymer or due to the phase transition. A similar phenomenon was found in a comparable system by Weisenburger and Koenig[20] using the same imaging technique.

Figure 3 shows three stacked plots of the signal intensity of semiprofiles stretching from the center of the polystyrene cylinder to the bulk dioxane in the test tube. The figures indicate the time (in minutes) elapsed after exposure to dioxane. The plateau to the right is the signal of the bulk dioxane; the inverted spike is the susceptibility artifact with the diffusion gradient to the left of it. The low plateau of the untouched polystyrene is at the extreme left. These plots allow a quantitative comparison of the three samples.

Although possible T_2 effects of dioxane fractions may be present at the leading edge of the advancing diffusion front, they will not seriously effect the measured diffusion profiles. The spatial extension of these strongly bound solvent molecules is considered to be very small, most likely below the pixel resolution. To avoid any contributions in the signal from the solvent itself, the polystyrene rods were allowed to swell in deuterated dioxane, producing measurements of line widths in the range of 600–800 Hz. This corresponds to a T_2* well below 1 ms, indicating a negligible contribution by the swollen polymer chains themselves.

In Figure 4, the diffusion distance is plotted versus time. The depth of penetration is measured as the difference between the original radius of the cylinder (4 mm) and the radius of the unswollen part of the sample. We defined a distinct threshold intensity value (corresponding to a certain solvent concentration) and monitored its spatial advance. The curves give a good estimation of the frontal velocity. In the case of the 5% cross-linked polystyrene, which shows linear behavior, this velocity is 27 nm/s. We are aware of the fact that there is a potential error in these values due to the flattening of the concentration gradient.

A remarkable feature of the penetration is its geometric homogeneity, with the circular shape of the front persisting

Table 1. $T_{1\rho H}$ Values (ms) of Unswollen Polystyrene and Polystyrene Swollen in Dioxane[a]

cross-link	q	o,m,p (■)	aliphatic CH_2 (*)	aliphatic CH (○)
	(a) Unswollen Polystyrene			
1%	4.6 ± 0.3	4.8 ± 0.3	4.6 ± 0.3	4.7 ± 0.3
2.5%	5.8 ± 0.4	5.5 ± 0.3	5.6 ± 0.3	5.6 ± 0.3
5%	6.7 ± 0.3	6.4 ± 0.3	6.5 ± 0.3	6.7 ± 0.3
	(b) Polystyrene Swollen in Dioxane			
1%		22.4 ± 2.5	14.9 ± 1.5	11.5 ± 1.2
2.5%	8.2 ± 0.9	9.2 ± 0.7	7.6 ± 0.6	4.1 ± 0.3
5%	1.4 ± 0.1	2.2 ± 0.1	1.6 ± 0.1	1.4 ± 0.1

[a] q quaternary aromatic peak at 146 ppm, o,m,p (■) aromatic peak at 128 ppm, (*) aliphatic methylene peak at 46 ppm, and (o) aliphatic methyne peak at 40 ppm.

until the core of the sample is reached. There are no inner voids or stress cracks visible, indicating the high quality of the material.

The process of the uptake of fluid in polymers is an extremely complex problem, with the osmotic pressure and the swelling forces interacting in a complex way. The stacked plots of the diffusion profiles demonstrate the consequences of cross-linking upon the shape of the solvent gradient. The concentration profile of dioxane in 1% cross-linked polystyrene shows a steep gradient which advances in time toward the center of the cylinder and which retains its slope throughout the process. This gradient is followed by a plateau in the outer region of the polymer which can be correlated to the so-called case II type of diffusion. Case II diffusion normally occurs when strong interactions between polymer and solvent exist.

With 5% cross-linked polystyrene, the initial steep gradient at the surface of the sample gradually flattens in time, typically of Fickian diffusion.

The behavior of 2.5% cross-linked polystyrene lies between these two extremes, showing elements of both diffusion types. Thus, a slight variation in the degree of cross-linking of polystyrene results in a profound change of the diffusion characteristics.

As expected, the velocity of the advancing front is also dependent upon the degree of cross-linking, with 1% cross-linked polystyrene being the fastest, followed in succession by the 2.5% and 5% material.

The swelling curves of the polymers correspond approximately to the diffusion velocities. Both the rate and the extent of swelling were greatest for 1% cross-linked polystyrene.

A quantitative evaluation of the diffusion constants is currently under way. Because different parameters influence the diffusion process, only a precise simulation of the diffusion curves will yield accurate values.

3.2. Solid-State NMR Investigations. $T_{1\rho H}$ values for unswollen and swollen polystyrene which are sensitive to motions in the kilohertz motional regime are summarized in Table 1.

In glassy polymers decreasing $T_{1\rho H}$ values can be correlated to increasing mobility.[21] On the basis of $T_{1\rho H}$ values, it is apparent that for unswollen polystyrene the highest mobility is found for 1% cross-linked material (Table 1a). The fact that the spin-diffusion process is efficient and the average mobility of the sample can be described by one $T_{1\rho H}$ indicates that the polymer is homogeneous. Swelling of the polymer in dioxane is accompanied by decreasing $T_{1\rho H}$ values, indicating a decrease in mobility, as is also confirmed by temperature-dependent relaxation measurements. Spin diffusion is no longer a dominant process (Table 1b), indicating that

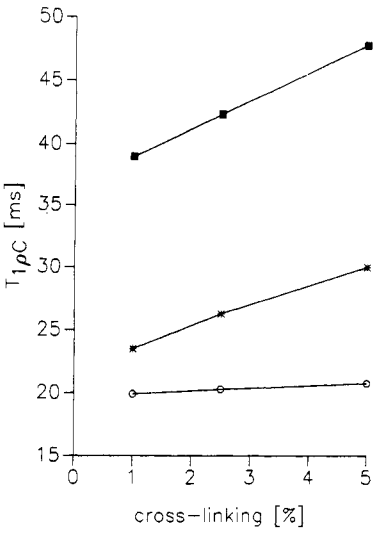

Figure 5. Plot of $T_{1\rho C}$ (ms) versus the degree of cross-linking of unswollen polystyrene. Only the data from the mobile carbon fraction has been plotted. The rotating field was 32 kHz. (■) o,m,p phenyl group at 128 ppm, (*) aliphatic CH_2 group at 46 ppm, and (○) aliphatic CH at 40 ppm.

motion is sufficiently rapid to average the direct C–H and H–H dipolar interactions; $T_{1\rho H}$ is now determined by local motions.

Although cross-polarization is an inefficient process for polymers in the gel state since the static dipolar interaction necessary for efficient cross-polarization has been eliminated or greatly reduced, C–H cross-polarization can be established. Thus, the ability to obtain a CP spectrum and to measure $T_{1\rho H}$ of the swollen samples suggests that at least a small residual component of the static dipolar interaction remains.[27] In addition, CP also may occur via a reduced dipolar broadening by molecular motion.[27]

The highest $T_{1\rho H}$ values for the o, m, p aromatic peak indicate that maximum mobility of the phenyl group is found in the gel state, whereby this effect is most dominant for the 1% cross-linked polystyrene. $T_{1\rho H}$ is controlled by these slow phenyl group motions for which the kilohertz frequency motional regime is sensitive.[28]

To gain more information on the local motions in the mid-kilohertz regime in the glassy state, we performed $T_{1\rho C}$ measurements (Table 2). Measurements in the gel state are not shown because the poor signal-to-noise ratio makes the values inaccurate. Fortunately, $T_{1\rho H}$ can be used instead as a parameter to describe local motions in swollen polystyrene.

There are always two $T_{1\rho C}$ values: the lower one is correlated to carbons with a reduced mobility, compared to those with higher values and higher mobility.[30] Figure 5 shows a plot of $T_{1\rho C}$ of the more mobile carbon fraction versus the amount of cross-linking. The values of the quaternary carbon atoms have been omitted, since these carbons have no directly bonded protons and relax indirectly via the aromatic protons.

With increasing cross-linking $T_{1\rho C}$ increases and mobility decreases. The phenyl groups (■) of the glassy polymer exhibit in the mid-kilohertz regime at 32 kHz a reduced mobility relative to the gel state (Table 1b). It is interesting to note that the mobility of the aliphatic methylene groups changes only slightly with a density of cross-linking in the range 1–5%.

The two $T_{1\rho C}$ values represent different long-range torsional oscillations of the phenyl groups as part of different main-chain motions locked into the glassy polymer by inter- and intrachain steric interactions.[21] They

Table 2. $T_{1\rho C}$ Values (ms) of Unswollen Polystyrene[a]

cross-link	q		o,m,p (■)		aliphatic CH_2 (*)		aliphatic CH (○)	
1%	3.0 ± 0.3	61 ± 3	2.3 ± 0.1	39 ± 2.3	1.3 ± 0.6	19.9 ± 1.2	1.7 ± 0.1	23.5 ± 1.8
2.5%	3.7 ± 0.3	68 ± 2.7	2.4 ± 0.4	42 ± 2.1	1.5 ± 0.07	20.3 ± 1.1	1.6 ± 0.2	26.3 ± 2.0
5%	5.0 ± 0.3	77 ± 4.6	2.7 ± 0.1	48 ± 1.9	1.6 ± 0.06	20.8 ± 0.8	4.0 ± 0.36	30.1 ± 2.7

[a] q quaternary aromatic peak at 146 ppm, o,m,p (■) aromatic peak at 128 ppm, (*) aliphatic methylene peak at 46 ppm, and (o) aliphatic methyne peak at 40 ppm.

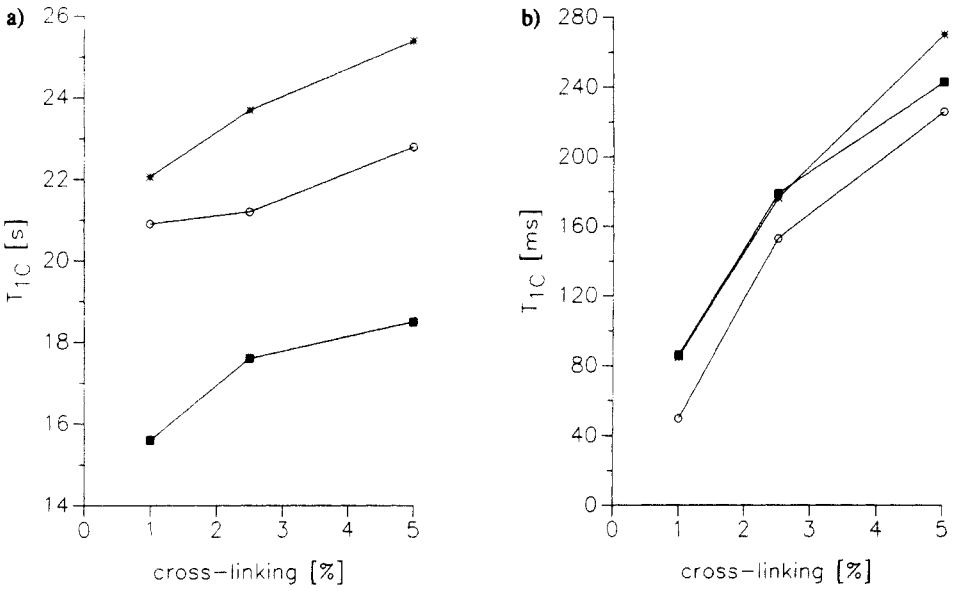

Figure 6. Plot of T_{1C} versus the degree of cross-linking of (a) unswollen polystyrene and (b) polystyrene swollen in dioxane. (■) o,m,p phenyl group at 128 ppm, (*) aliphatic CH_2 group at 46 ppm, and (○) aliphatic CH at 40 ppm.

Table 3. T_{1C} Values of Unswollen Polystyrene[a]

cross-link	q	o,m,p (■)	aliphatic CH_2 (*)	aliphatic CH (○)
	(a) Unswollen Polystyrene (in s)			
1%	30.5 ± 2.1	15.6 ± 0.9	20.9 ± 1.3	22.0 ± 1.8
2.5%	32.7 ± 2.6	17.6 ± 1.0	21.2 ± 1.3	23.7 ± 1.9
5%	34.4 ± 2.5	18.5 ± 1.1	22.8 ± 1.2	25.4 ± 2.3
	(b) Polystyrene Swollen in Dioxane (in ms)			
1%	b	86 ± 9	49.7 ± 4.3	84.9 ± 8
2.5%	b	147.9 ± 13	153 ± 12.2	176 ± 12.3
5%	b	243 ± 16.7	226 ± 13.5	270 ± 21.6

[a] q quaternary aromatic peak at 146 ppm, o,m,p (■) aromatic peak at 128 ppm, (*) aliphatic methylene peak at 46 ppm, and (○) aliphatic methyne peak at 40 ppm. [b] It was impossible to determine T_{1C} of the quaternary carbons accurately, since these atoms were barely detectable in the gel state.

indicate that the rings and main chains of the polystyrenes assume various frozen conformations and configurations with motions in the range of several 100 kHz and do not rapidly interconvert.[20,29] The low $T_{1\rho C}$ values reflect restricted phenyl rotations with a low-frequency small amplitude due to certain intrachain interactions.[20]

Information upon the dynamic behavior in the megahertz-frequency range can be obtained by T_{1C} measurements, the values of which are presented in Table 3a,b and Figure 6a,b. The values of the quaternary carbons have been omitted; the low signal-to-noise ratio of these groups in the gel state precluded their accurate determination.

In contrast to $T_{1\rho C}$, there is a monoexponential decay of T_{1C} in the glassy state and in the gel state. Table 3a shows that there is a similar dependence of the motional behavior of all groups upon the degree of cross-linking (Figure 6a), and thus increasing mobility can be correlated with decreasing T_{1C}; the samples with 5% cross-links have the lowest mobility. The phenyl groups (■) exhibit in the megahertz-motional regime the highest mobility. After swelling, mobility increases dramatically and the whole system becomes extremely flexible. The relaxation behavior of all groups of polystyrene with a given degree of cross-linking is similar. That means that solvation equalizes the effects of individual mobility and that the polymers must have a homogeneous frequency distribution of motion. In addition, the differences in mobility between the 1% and 5% cross-linked materials are significantly greater in the gel state than in the glassy state (Figure 6b).

In summary we conclude, on the basis of relaxation measurements, that there are no great differences in the megahertz or average kilohertz motions (measured by T_{1C} or $T_{1\rho H}$) between the various cross-linked polystyrenes in the swollen state. No predominant features are apparent in the $T_{1\rho C}$ values (describing local kilohertz motions) which would readily explain the different diffusion behavior of the various polystyrenes. Thus, the findings revealed by NMRI can only be explained by dramatic changes in the dynamic behavior of the polymers induced by swelling upon transition from the glassy state into the gel state. This is revealed by the reduction of the T_{1C} values from 15–35 s to 50–270 ms. In the gel state motional dynamic differences between the 1% and 5% cross-linked polymers are apparent, from the 4-fold higher T_{1C} values of the latter polymers. Thus, higher T_{1C} values can be correlated with lower mobility; this fact has been confirmed by temperature-dependent measurements.[38]

The kilohertz mobilities are also strongly affected by the swelling process, and their amplitudes are significantly increased, which can be seen by the $T_{1\rho H}$ data obtained (Table 1b). The very high phenyl group mobility may be responsible for the strong interaction of dioxane with the polymer. This may explain the occurrence of case II diffusion. The velocity of the diffusion front (Figure 2) does not seem to be affected by these interactions but

seems to be dominated by the overall mobility of the samples.

References and Notes

(1) Benson, J. R.; Woo, D. J. *J. Chromatogr. Sci.* **1984**, *22*, 386.
(2) Bayer, E.; Schumann, W. *J. Chem. Soc., Chem. Commun.* **1986**, 949.
(3) Manecke, G.; Ehrental, E.; Schlünsen, J. In *Characterization of Immobilized Biocatalysts*; Buchholz, K., Ed.; Schön & Wetzel: Frankfurt, FRG, 1979; p 49.
(4) Chibata, J. *Immobilized Enzymes*; Wiley: New York, 1978, p 9.
(5) Daly, W. H. *Makromol. Chem. Suppl.* **1979**, *180*, 3.
(6) Grimshaw, R. W.; Holland, C. F. *Ion-Exchange: Introduction to Theory and Practice*; The Chemical Society: London, 1975.
(7) Merrifield, R. B. *J. Am. Chem. Soc.* **1963**, *85*, 2149.
(8) Bayer, E. *Angew. Chem., Int. Ed. Engl.* **1991**, *30*, 113.
(9) Bayer, E.; Rapp, W. In *Poly(Ethylene Glycol) Chemistry*; Harris, J. M., Ed.; Plenum Press: New York, 1992; p 325.
(10) Chung, D. Y. D.; Bartholini, M.; Guyot, A. *Angew. Makromol. Chem.* **1982**, *103*, 109.
(11) Ford, W. T.; Lee, J. L.; Tomoi, M. *Macromolecules* **1982**, *15*, 1246.
(12) Wehrli, F. W., Shaw, D., Kneeland, J. B., Eds. *Biochemical Resonance Imaging: Principles, Methodology and Applications*; VCH Publishers: New York, 1988.
(13) Kuhn, W. *Angew. Chem., Int. Ed. Engl.* **1990**, *29*, 1.
(14) Blümich, B., Kuhn, W., Eds. *Magnetic Resonance Microscopy*; VCH: Weinheim, Germany, 1992.
(15) Blümich, B. *Angew. Chem., Int. Ed. Engl.* **1988**, *27*, 1406; *Angew. Chem. Adv. Mater.* **1988**, *100*, 1460.
(16) Blümich, B.; Hagemeyer, A.; Schaefer, D.; Schmidt-Rohr, K.; Spiess, W. *Adv. Mater.* **1990**, *2*, 72.
(17) Günther, U.; Albert, K.; Grossa, M. *J. Magn. Reson.* **1992**, *98*, 593.
(18) Komoroski, R. A. *Anal. Chem.* **1993**, *65*, 1068A.
(19) Rothwell, W. P.; Gentempo, P. P. *Bruker Report* **1985**, *1*, 46.
(20) Weisenburger, L. A.; Koenig, J. *Polym. Prepr. (Am. Chem. Soc., Div. Polym. Chem.)* **1988**, *29*, 98.
(21) Blackband, S.; Mansfield, P. *J. Phys. C* **1986**, *19*, L49.
(22) Bayer, E.; Müller, W.; Ilg, M.; Albert, K. *Angew. Chem., Int. Ed. Engl.* **1989**, *28*, 1029; *Angew. Chem.* **1989**, *101*, 1033.
(23) Ilg, M.; Maier-Rosenkranz, J.; Müller, W.; Albert, K.; Bayer, E. *J. Magn. Reson.* **1992**, *96*, 335.
(24) Ford, W. S.; Balakrishnan, T. *Macromolecules* **1981**, *14*, 284.
(25) Bayer, E.; Albert, K.; Willisch, H.; Rapp, W.; Hemmasi, B. *Macromolecules* **1990**, *23*, 1937.
(26) Schaefer, J.; Stejskal, E. O.; Buchdahl, R. *Macromolecules* **1977**, *10*, 384.
(27) Steger, T. R.; Schaefer, J.; Stejskal, E. O.; McKay, R. A. *Macromolecules* **1980**, *13*, 1127.
(28) Stejskal, E. O.; Schaefer, J.; Sefcik, M. D.; McKay, R. A. *Macromolecules* **1981**, *14*, 275.
(29) Komoroski, R. A. *High Resolution NMR Spectroscopy of Synthetic Polymers in Bulk*; VCH Publishers: New York, 1986.
(30) Ganapathy, S.; Chacka, V. P.; Bryant, R. G. *Macromolecules* **1986**, *19*, 1021.
(31) Schaefer, J.; Sefcik, M. D.; Stejskal, E. O.; McKay, R. A.; Dixon, W. T.; Cais, R. E. *Macromolecules* **1984**, *17*, 1107.
(32) Elifore, L. A.; Cooper, S. L. *Polymer* **1984**, *25*, 645.
(33) Ford, W. T.; Periyasamy, M.; Mohanraj, S. *J. Polym. Sci., Polym. Chem.* **1989**, *27*, 2345.
(34) Periyasamy, M.; Ford, W. T.; McEnroe, F. J. *J. Polym. Sci., Polym. Chem.* **1989**, *27*, 2357.
(35) Schaefer, J.; Stejskal, E. O.; Buchdahl, R. J. *Macromol. Sci. Phys.* **1977**, *13* (4), 665.
(36) Sullivan, M. J.; Maciel, G. E. *Anal. Chem.* **1982**, *54*, 1615.
(37) Haase, A.; Frahm, J.; Matthaei, D.; Merboldt, K. D.; Hänicke, W. *J. Magn. Reson.* **1986**, *67*, 217.
(38) Buxton, R.; Fisel, C.; Chien, D.; Brady, T. *J. Magn. Reson.* **1989**, *83*, 576.